Rawafed Almarefa Journal مجلة روافد المعرفة
ISSN: 2709-0345 Volume: 07, Issue: 13, (2026), Pages: 155-173

Oblique Traveling-Wave Solutions of a $(2+1)$-Dimensional Whitham–Broer–Kaup System: a KP-Type Extension

*Ramadan M. Al − Naas Al − Wahishi*1 *and Ragab M. A. Almasroub*1,*

1-Department of Mathematics, Faculty of Science, Azzyatuna University
Email:mariamlamya62@gmail.com
Email:almasrovb4392@gmail.com
Received: 02-11-2026; Accepted: 07-11-2026; Published: 29-00-2026

Abstract

This paper is a companion to our study of the exact traveling-wave solutions of the $(1+1)$-dimensional Whitham–Broer–Kaup (WBK) system (Almasroub & Al-Naas Al-Wahishi, 2026), and carries out the $(2+1)$-dimensional extension left as future work. Several inequivalent $(2+1)$-dimensional WBK generalizations exist in the literature (Ali & Younas, 2025; Pashaev & Rogers, 2025; Zheng et al., 2005); rather than reproduce any one of them, we define, explicitly and self-containedly, a specific anisotropic Kadomtsev–Petviashvili (KP)-type extension (Kadomtsev & Petviashvili, 1970) in which a single nonlocal term $\sigma\,\partial_x^{-1}u_{yy}$ is added to the mass-balance equation, with the operator ∂_x^{-1} fixed on precisely specified function classes; the system reduces to the original WBK system exactly when the transverse derivative vanishes. Under an oblique traveling-wave ansatz $\xi = x + \ell y - ct$, we prove that the reduction is governed by exactly the same second-order ODE solved in Almasroub and Al-Naas Al-Wahishi (2026), with the integration constant C_1 replaced throughout by $C_1' := C_1 + \sigma\ell^2$ ($\sigma = \pm 1$ the KP sign, ℓ the transverse wavenumber), while the free-surface field itself retains the original C_1. Consequently, each of the ten independent Jacobi-elliptic families extends, without further computation, to an exact oblique-wave solution of the $(2+1)$-dimensional system, with c replaced by $\tilde{c} = \sqrt{c^2 + 2C_1 + 2\sigma\ell^2}$ in the amplitudes; real amplitudes require $\tilde{c}^{\,2} > 0$, i.e. $\ell^2 < (c^2 + 2C_1)/2$ when $\sigma = -1$. We state the amplitude sign rule in a branch-independent form, which corrects the sign of the complex branch of Case 4. All ten families are verified to 50-digit precision directly against the original, unintegrated $(2+1)$-dimensional PDE system – not merely the reduced ODE – by a multi-period grid scan for both signs of σ. Setting $\ell = 0$ recovers every result of Almasroub and Al-Naas Al-Wahishi (2026) identically.

Keywords: (2 + 1)-dimensional Whitham–Broer–Kaup system; Kadomtsev–Petviashvili-type extension; oblique traveling waves; Jacobi elliptic functions; exact solutions.

الملخص

تُعدّ هذه الورقة مكمِّلةً لدراستنا السابقة للحلول الموجية المتنقلة الدقيقة لنظام وايتهام–برووير–كاوب (WBK) في البعد $(1+1)$ (Almasroub & Al-Naas Al-Wahishi, 2026)، وتُنجز التعميم إلى البعد $(2+1)$ الذي تُرك هناك عملاً مستقبلياً. نعرّف صراحةً امتداداً غير متناحٍ من نوع كادومتسيف–بتفياشفيلي (KP) يُضاف فيه حدٌّ غير محلي وحيد

This is an open access article under the CC BY-SA license.

$\sigma\ \partial_x^{-1}u_{yy}$ إلى معادلة حفظ الكتلة، مع تحديدٍ دالّيٍّ دقيقٍ للمؤثر ∂_x^{-1}، ويؤول النظام إلى نظام WBK الأصلي تماماً عند انعدام الاعتماد العرضي. وباستعمال المتغير المائل $\xi = x + \ell y - ct$ نبرهن أن الاختزال تحكمه المعادلة التفاضلية العادية من الرتبة الثانية نفسها المحلولة في الدراسة السابقة، مع استبدال ثابت التكامل C_1 بالثابت $C_1' = C_1 + \sigma\ell^2$، حيث $\sigma = \pm 1$ إشارة KP و ℓ العدد الموجي المستعرض، بينما يحتفظ حقل السطح الحر بالثابت الأصلي C_1. وبناءً عليه تمتد كل عائلة من العائلات الجاكوبية العشر المستقلة إلى حلٍّ موجيٍّ مائلٍ دقيقٍ في البعد $(2+1)$، مع استبدال c بالمقدار $\tilde{c} = \sqrt{c^2 + 2C_1 + 2\sigma\ell^2}$ في السعات؛ وتتطلب السعات الحقيقية الشرط $\tilde{c}^{\,2} > 0$، أي $\sigma = -1$ عندما $\ell^2 < (c^2 + 2C_1)/2$. كما نصوغ قاعدة إشارة السعات بصيغة مستقلة عن الفرع، تُصحّح إشارة الفرع المركّب للحالة الرابعة، ونتحقق من العائلات العشر جميعها بدقة 50 رقماً عشرياً مباشرةً على نظام المعادلات التفاضلية الجزئية الأصلي غير المكامَل عبر مسحٍ شبكيٍّ يغطي عدة دورات ولكلتا إشارتي σ. وعند $\ell = 0$ تُستعاد جميع نتائج الدراسة السابقة تماماً.

الكلمات المفتاحية: *نظام وايتهام–بروير–كاوب في البعد (2+1)؛ امتداد من نوع كادومتسيف–بتفياشفيلي؛ موجات متنقلة مائلة؛ دوال جاكوبي الإهليلجية؛ حلول دقيقة.*

1 Introduction

In the companion paper (Almasroub & Al-Naas Al-Wahishi, 2026) constructed and rigorously verified ten algebraically independent exact traveling-wave families for the $(1+1)$-dimensional Whitham–Broer–Kaup system

$$u_t + u\,u_x + v_x + b\,u_{xx} = 0, \tag{1}$$

$$v_t + (uv)_x + a\,u_{xxx} - b\,v_{xx} = 0, \tag{2}$$

and explicitly left the $(2+1)$-dimensional generalization as a direction for future research.

A wide range of analytical techniques has been developed for constructing exact traveling-wave solutions of nonlinear partial differential equations of this type, including the first-integral method (Abdoon, 2015; El-Sabbagh & El-Ganaini, 2012), the Exp-function method (El-Borai et al., 2015; He, 2013), the functional variable method (Zerarka et al., 2010; Zerarka et al., 2016), the Jacobi elliptic function method (Gepreel, 2014; Maruno et al., 2003), the tanh-function method (El-Borai & Al-Masroub, 2015; Parkes, 2010; Wazwaz, 2007), the (G'/G)-expansion method (Almasroub et al., 2020; Kumar & Chand, 2014; Zheng, 2013), the $(G'/G, 1/G)$-expansion method (Al-shawba et al., 2018), the Kudryashov method (Zayed & Alurrfi, 2014; Zayed & Alurrfi, 2015), the generalized Riccati mapping method (El-Borai et al., 2016; Li et al., 2014), and dynamical reduction approaches (Seadawy et al., 2025; Zhang et al., 2008); the generalized F-expansion method used in Almasroub and Al-Naas Al-Wahishi (2026) and here, and the closely related elliptic equation rational expansion method (Chen et al., 2005), belong to the same broad family of auxiliary-equation techniques, in which the traveling-wave profile is expanded in a function satisfying a simpler, explicitly solvable ordinary differential equation. For the specific $(2+1)$-dimensional setting, there is no single, universally agreed $(2+1)$-dimensional WBK system in the literature: distinct constructions based on Painlevé–Bäcklund reduction (Zheng et al., 2005), on Lax-pair or resonant-NLS connections (Pashaev & Rogers, 2025), and on other extended auxiliary-equation approaches (Ali & Younas, 2025) all

This is an open access article under the CC BY-SA license.

carry the name "$(2+1)$-dimensional Whitham–Broer–Kaup system" while being genuinely different equations. Rather than assert equivalence with any one of these, we define our own extension explicitly in Section 2, using the same weak-transverse-dependence (Kadomtsev–Petviashvili, KP) mechanism by which the Korteweg–de Vries equation is classically extended to the KP equation (Ablowitz & Segur, 1979; Kadomtsev & Petviashvili, 1970): a single nonlocal term $\sigma\ \partial_x^{-1}u_{yy}$ is added to the mass-balance equation, and the resulting system reduces to (1)–(2) exactly when $\partial_y \equiv 0$.

Relation to integrable KP methods and other multidimensional WBK models

It is useful to situate the present approach structurally. For the KP equation itself, the integrable machinery – Hirota's bilinear method (Hirota, 2004), the Wronskian technique (Freeman & Nimmo, 1983), and Darboux transformations (Matveev & Salle, 1991) – generates interacting multi-line solitons and resonant web patterns (Kodama, 2010), algebraically decaying lump solutions (Satsuma & Ablowitz, 1979), and breather-type solutions, including solutions on periodic (elliptic) backgrounds. These constructions rely on the integrable structure (Lax pair, bilinear form, τ-function). The auxiliary-equation approach used here is structurally and methodologically different: it requires no integrability – and none is claimed for the model below – and it produces compact closed-form *algebraic* families confined to the oblique traveling-wave sector, i.e. to solutions depending on the single phase $\xi = x + \ell y - ct$. It therefore cannot produce interacting line solitons, lumps or breathers, which require two or more phases or genuinely non-planar structure; conversely, within its sector it delivers the complete ten-family Jacobi-elliptic classification in explicit form. We also stress the *anisotropic* character of the model: exactly as in the classical passage from KdV to KP through the operator $\partial_x^{-1}\,\partial_y^2$, the transverse direction enters only through a weak, nonlocal correction to propagation that is predominantly along x, so that x and y do not play symmetric roles. This distinguishes the present system from isotropic or fully two-dimensional WBK generalizations, such as those connected with resonant NLS and Davey–Stewartson-type systems (Davey & Stewartson, 1974; Pashaev & Rogers, 2025), and from fully dispersive KP-type extensions.

The main result of this paper (Theorem 1) is that the oblique traveling-wave reduction of this system is not a new solvable problem: it is exactly the general-C_1 problem already solved in (Almasroub & Al-Naas Al-Wahishi, 2026), with a specific, explicit substitution for C_1. Every exact family constructed there therefore extends immediately to a genuine, non-degenerate $(2+1)$-dimensional exact solution – and we verify this extension directly against the original PDE system, not only the reduced ODE.

Remark 1 (Scope and novelty). To state precisely what is new here and what is inherited: the ten Jacobi auxiliary families themselves are inherited from (Almasroub & Al-Naas Al-Wahishi, 2026); this paper does not produce a new, independent one-dimensional reduced ODE, since Theorem 1 establishes exact equivalence with the previous general-C_1 ODE after the parameter substitution $C_1' = C_1 + \sigma\ell^2$. The phrase "ten new Jacobi elliptic solution families" would therefore overstate the contribution; the precise claim is that we construct and verify exact $(2+1)$-dimensional oblique extensions of the ten previously classified Jacobi-elliptic traveling-wave families. What is new is the explicit KP-type $(2+1)$-dimensional model itself, with a precise functional definition of its nonlocal term (Section 2); the reduction theorem

This is an open access article under the CC BY-SA license.

linking its oblique sector to the previously solved class, with all admissibility conditions stated explicitly (Theorem 1); a branch-independent amplitude sign rule that corrects the complex branch of Case 4 (Section 4); the resulting genuinely two-dimensional wave geometry – oblique wavefronts, pole lattices, multi-crest patterns, and localized packets in the (x, y)-plane (Section 6); and the direct high-precision verification of all ten families, by a multi-period grid scan for both signs of σ, against the full, unintegrated $(2 + 1)$-dimensional PDE (Section 5), which is a strictly stronger check than verifying the reduced ODE alone.

2 The $(2 + 1)$-Dimensional System

Proposition 1 (Definition of the extended system). Let $u = u(x, y, t)$, $v = v(x, y, t)$, and let $a, b \in \mathbb{R}$ be the dispersion parameters of (Almasroub & Al-Naas Al-Wahishi, 2026). Fix $\sigma \in \{+1, -1\}$. The $(2 + 1)$-dimensional system considered here is

$$u_t + u\,u_x + v_x + b\,u_{xx} = 0, \tag{3}$$

$$v_t + (uv)_x + a\,u_{xxx} - b\,v_{xx} + \sigma\,\partial_x^{-1}u_{yy} = 0. \tag{4}$$

The nonlocal operator ∂_x^{-1} is defined on the following two function classes (all functions smooth, or meromorphic in x, with x-derivatives of all orders):

(i) *Decaying class* $\mathcal{D}$: $w(\cdot, y, t)$ and its x-derivatives tend to zero as $x \to -\infty$; then

$$\partial_x^{-1}w(x, y, t) \coloneqq \int_{-\infty}^{x} w\,(s, y, t)\,ds.$$

(ii) *Periodic mean-zero class* $\mathcal{P}_0$: $w(\cdot, y, t)$ is L-periodic in x with zero mean, $\frac{1}{L}\int_{x_0}^{x_0+L} w\,dx = 0$ (for functions with real poles the mean is taken along a pole-free line $\mathrm{Im}x = \delta \neq 0$, which by periodicity and Cauchy's theorem is independent of δ); then $\partial_x^{-1}w$ is the *unique* L-periodic antiderivative of w with zero mean.

In both classes $\partial_x^{-1}\,\partial_x w = w$, the operator acts trivially (as the zero operator) on functions independent of x, and no arbitrary function of integration $h(y, t)$ can arise. Equivalently, (4) can be written in the local form

$$\partial_x[v_t + (uv)_x + a\,u_{xxx} - b\,v_{xx}] + \sigma\,u_{yy} = 0, \tag{5}$$

supplemented by the above normalization, which removes the x-independent constant of integration. System (3)–(4) reduces to (1)–(2) exactly when u, v are independent of y.

Remark 2 (Physical and asymptotic motivation for placing the transverse term in (4)). In the classical shallow-water reading of the WBK system (Kaup, 1975; Whitham, 1974), u is the horizontal velocity, v the free-surface elevation (local depth), (1) is the momentum balance and (2) the mass balance. Introduce a weak transverse velocity w under the standard KP scaling $\partial_y = O(\varepsilon)\,\partial_x$, $w = O(\varepsilon)\,u$ (Ablowitz & Segur, 1979; Kadomtsev & Petviashvili, 1970). Irrotationality, $u_y = w_x$, gives $w = \partial_x^{-1}u_y$. In the mass balance the transverse flux contributes

This is an open access article under the CC BY-SA license.

$\partial_y(v\,w)$, whose leading part about a background level v_0 is $v_0\,\partial_x^{-1}u_{yy} = O(\varepsilon^2)$ – the same order as the weak-dispersion terms retained in the KP balance. In the momentum balance, by contrast, the only transverse contribution is the advective term $w\,u_y$, which is quadratic in the small amplitude and of higher order. Rescaling y to normalize $|v_0|$ yields the single term $\sigma\ \partial_x^{-1}u_{yy}$ in (4), with $\sigma = \mathrm{sign}(v_0)$; $\sigma = +1$ is the case of a positive background, and $\sigma = -1$ is retained as the formal counterpart (the analogue of the two sign choices of KP). The placement is also consistent with conservation laws: with $w = \partial_x^{-1}u_y$, (4) is the two-dimensional conservation law

$$v_t + \partial_x(uv + a\,u_{xx} - b\,v_x) + \partial_y(\sigma\,w) = 0,$$

so that $\iint v\,dx\,dy$ is conserved in the classes $\mathcal{D}, \mathcal{P}_0$, while (3) keeps its conservation form $u_t + \partial_x\left(\frac{1}{2}u^2 + v + b\,u_x\right) = 0$. We emphasize that this is a formal weakly-transverse argument, not a complete asymptotic derivation from the Euler equations, and we do not claim a Hamiltonian structure for (3)–(4). Finally, as Theorem 1 shows, this placement is also the one for which the oblique reduction stays a second-order ODE of the same algebraic type as in (Almasroub & Al-Naas Al-Wahishi, 2026). Placing the term in (3) instead changes the reduced ODE in three coefficients at once – it introduces a first-derivative term $b\sigma\ell^2U'$ and also shifts the coefficients of U^2 and U – and a parity obstruction then excludes every non-constant solution of the rational Jacobi-elliptic form; this alternative is documented in full in Appendix A.

3 Oblique Reduction

Let $\ell \in \mathbb{R}$ (the transverse wavenumber) and $c > 0$, and set

$$\xi := x + \ell y - ct, \qquad u(x,y,t) = U(\xi), \qquad v(x,y,t) = V(\xi). \tag{6}$$

Then $\partial_x = \partial_\xi$, $\partial_y = \ell\ \partial_\xi$, $\partial_t = -c\ \partial_\xi$, and consequently $u_{yy} = \ell^2 U''(\xi)$.

Lemma 1 (Realization of nonlocal term): If U is L-periodic (as for every family of Section 4, L being a real or complex period of F), or if U' belongs to $\mathcal{D}$, then

$$\partial_x^{-1}u_{yy} = \ell^2 U'(\xi), \tag{7}$$

uniquely.

Proof. In the periodic case $u_{yy} = \ell^2 U''(\xi)$ is the x-derivative of the periodic function $\ell^2 U'(\xi)$, hence has zero mean and lies in $\mathcal{P}_0$; and U' itself has zero mean because it is the derivative of the periodic function U. Hence $\ell^2 U'$ is the unique zero-mean periodic antiderivative of u_{yy}. In the decaying case, $\int_{-\infty}^{x} \ell^2\,U''\,ds = \ell^2 U'$ directly. ▫

Equation (3) is unchanged in form from the $(1+1)$-dimensional case; integrating it once, exactly as in (Almasroub & Al-Naas Al-Wahishi, 2026), gives

$$V(\xi) = c\,U(\xi) - \tfrac{1}{2}U^2(\xi) - b\,U'(\xi) + C_1, \tag{8}$$

This is an open access article under the CC BY-SA license.

with C_1 a free integration constant, unaffected by ℓ or σ, since the transverse term does not appear in (3).

Throughout, (l_0, l_1, l_2) are the coefficients of the auxiliary equation $F'^2 = l_0 + l_1F^2 + l_2F^4$ of (Almasroub & Al-Naas Al-Wahishi, 2026), and

$$D := 6\sqrt{l_0 l_2} - l_1, \tag{9}$$

where $\sqrt{l_0 l_2}$ denotes one fixed determination of the root, the same one used in every formula below (it is listed explicitly for each family in Table 1).

Theorem 1 (Reduction to the general-C_1 problem). Substituting (8) and (7) into (4) and integrating once more gives

$$(a + b^2)\,U''(\xi) + \frac{3}{2}\,c\,U^2(\xi) - \frac{1}{2}\,U^3(\xi) + (C_1' - c^2)U(\xi) + C_2 = 0, \tag{10}$$

where

$$C_1' := C_1 + \sigma\ell^2. \tag{11}$$

Equation (10) is identical, term for term, to Eq. (35) of (Almasroub & Al-Naas Al-Wahishi, 2026) with its "C_1" read as C_1'. Consequently, let F be any family of Table 1, with data (l_0, l_1, l_2, D), and assume

(H1) $l_0 l_2 \neq 0$ and $D \neq 0$;

(H2) $\tilde{c}^{\,2} := c^2 + 2C_1' = c^2 + 2C_1 + 2\sigma\ell^2 > 0$, with $\tilde{c} > 0$;

(H3) the dispersion parameters are tied by $a + b^2 = \tilde{c}^{\,2}/(2D)$ (so that, for a given b, a is determined, and $\operatorname{sign}(a + b^2) = \operatorname{sign}(D)$ for real D).

Then the oblique reduction admits the exact solution

$$U(\xi) = c + g_1F(\xi) + \frac{f_1}{F(\xi)}, \qquad g_1 = \tilde{c}\sqrt{\frac{2l_2}{D}}, \qquad g_1 f_1 = \frac{2\,\tilde{c}^{\,2}\sqrt{l_0 l_2}}{D}, \tag{12}$$

with the integration constant

$$C_2 = -c\,C_1' = -c\,(C_1 + \sigma\ell^2), \tag{13}$$

where the root in (12) is the same determination of $\sqrt{l_0 l_2}$ as in (9), and $V(\xi)$ is given by (8) using the original C_1 (not C_1'). Setting $\ell = 0$ recovers Theorem 1 of (Almasroub & Al-Naas Al-Wahishi, 2026) exactly.

Proof. Differentiating (8), substituting into (4) together with (7), and expanding gives, after full simplification (carried out independently by computer algebra),

$$-cV' + (UV)' + aU''' - bV'' + \sigma\ell^2U'$$

$$= C_1U' + (a + b^2)U''' - c^2U' + 3c\,UU' + \sigma\ell^2U' - \frac{3}{2}U^2U'. \tag{14}$$

This is an open access article under the CC BY-SA license.

The right-hand side is $\frac{d}{d\xi}\left[(a+b^2)U'' + \frac{3}{2}cU^2 - \frac{1}{2}U^3 + (C_1 + \sigma\ell^2 - c^2)U\right]$; integrating once and calling the constant of integration $-C_2$ gives (10)–(11) exactly. Equation (10) depends on C_1, σ, ℓ only through the single combination $C_1' = C_1 + \sigma\ell^2$. Substituting $U = c + g_1F + f_1/F$, with $F'' = l_1F + 2l_2F^3$ and $F'^2 = l_0 + l_1F^2 + l_2F^4$, and multiplying by F^3, the coefficients of F^6, F^4, F^3, F^2, F^0 vanish if and only if

$$g_1^2 = 4(a+b^2)\,l_2, \qquad f_1^2 = 4(a+b^2)\,l_0, \qquad 3f_1g_1 = 2(a+b^2)\,l_1 + \tilde{c}^{\,2}, \qquad C_2 = -cC_1'.$$

The first two give $f_1g_1 = 4(a+b^2)\sqrt{l_0l_2}$ for one determination of the root; the third then gives $(a+b^2)\left(12\sqrt{l_0l_2} - 2l_1\right) = \tilde{c}^{\,2}$, i.e. (H3) with D as in (9), and hence (12). Setting $\ell = 0$ gives $C_1' = C_1$, recovering the original theorem exactly. This was also verified independently by direct symbolic expansion of (4) (not merely by the relabeling argument above). ▫

Remark 3 (Why the product rule). Writing $f_1 = \varepsilon\,\tilde{c}\sqrt{2l_0/D}$ with principal square roots, as was done for Case 4 in (Almasroub & Al-Naas Al-Wahishi, 2026), is correct only when ε is chosen so that the product condition in (12) holds. For real, positive $2l_0/D$ and $2l_2/D$ this means $\varepsilon = \mathrm{sign}\left(\sqrt{l_0l_2}/D\right)$; but when $2l_0/D$ and $2l_2/D$ are both negative, the two principal roots are both imaginary and their product carries an extra factor $i \cdot i = -1$. The product form $g_1f_1 = 2\tilde{c}^{\,2}\sqrt{l_0l_2}/D$ is branch-independent and removes this ambiguity; its consequence for Case 4 is made explicit in (19).

Remark 4 (Two independent constants). Unlike the $(1+1)$-dimensional case, C_1 (the background level of V, Eq. (8)) and C_1' (the coefficient entering the amplitude formulas (12)–(13)) are here generally different constants, related by (11). Setting $C_1 = 0$ – the zero-background choice of Almasroub and Al-Naas Al-Wahishi (2026, Remark 1) – does not give $C_1' = 0$ unless $\ell = 0$: it gives the purely-transverse case $C_1' = \sigma\ell^2$, $\tilde{c} = \sqrt{c^2 + 2\sigma\ell^2}$, $C_2 = -c\sigma\ell^2$, with V itself still background-free.

Remark 5 (Admissible parameter regimes and the case $\tilde{c}^{\,2} \le 0$). Hypothesis (H2) is automatic for $\sigma = +1$ whenever $c^2 + 2C_1 > 0$. For $\sigma = -1$ it imposes an explicit bound on the obliqueness,

$$\ell^2 < \ell_{\max}^2 := \frac{1}{2}(c^2 + 2C_1),$$

so that, for the KP sign $\sigma = -1$, wavefronts cannot be tilted beyond $\arctan\ell_{\max}$. The regimes violating (H2) are excluded from Theorem 1 as stated, and behave as follows. (a) If $\tilde{c}^{\,2} = 0$, then (H3) forces $a + b^2 = 0$, hence $g_1 = f_1 = 0$ and only the trivial constant state $U \equiv c$ survives. (b) If $\tilde{c}^{\,2} < 0$ (possible only for $\sigma = -1$ with $\ell^2 > \ell_{\max}^2$, or for sufficiently negative C_1), the coefficient identities in the proof of Theorem 1 still hold verbatim, since they involve $\tilde{c}$ only through $\tilde{c}^{\,2}$; but the reality pattern of the families is reversed, because $2\tilde{c}^{\,2}l_2/D$ changes sign. For example, Case 1 then becomes complex, while Case 4 on $0 < m < m^*$ (complex under (H2)) becomes *real*, with $a + b^2 = \tilde{c}^{\,2}/(2D) < 0$. We checked this numerically for Case 4 at $m = 0.5$, $c = 1.5$, $b = 0.6$, $C_1 = 0.3$, $\sigma = -1$, $\ell = 1.3$ (so $\tilde{c}^{\,2} = -0.53$): the solution

This is an open access article under the CC BY-SA license.

is real, with $g_1 \approx -0.55461$, $f_1 \approx 0.48030$, $a \approx -0.43690$, and both PDE residuals are below 10^{-50}. A systematic classification of this regime is left for future work.

4 The Ten Independent Oblique Families

Table 1 reproduces the auxiliary data of Table 1 in (Almasroub & Al-Naas Al-Wahishi, 2026) – unchanged, since (l_0, l_1, l_2, D) depend only on the choice of Jacobi function F, not on C_1, σ, ℓ – together with the determination of $\sqrt{l_0 l_2}$ used in (9). Table 2 records the resulting amplitudes under Theorem 1. Throughout, $\tilde{c} = \sqrt{c^2 + 2C_1 + 2\sigma\ell^2}$, $m \in (0,1)$ is the elliptic modulus, and

$$m^* := 2\sqrt{3\sqrt{2} - 4} \approx 0.985171431 \tag{15}$$

is the unique root in $(0,1)$ of $6\sqrt{1-m^2} = 2 - m^2$, i.e. of $D = 0$ for Cases 4–5 (it solves $m^4 + 32m^2 - 32 = 0$); thus $D > 0$ for $m < m^*$ and $D < 0$ for $m^* < m < 1$.

Table 1. *Auxiliary data of the ten families: $F'^2 = l_0 + l_1 F^2 + l_2 F^4$ and $D = 6\sqrt{l_0 l_2} - l_1$ (identical to Table 1 of Almasroub and Al-Naas Al-Wahishi (2026)).*

Case	$F(\xi)$	l_0	l_1	l_2	$\sqrt{l_0 l_2}$	D
1	sn	1	$-(1+m^2)$	m^2	m	$m^2 + 6m + 1$
2	cd	1	$-(1+m^2)$	m^2	m	$m^2 + 6m + 1$
3	cn	$1-m^2$	$2m^2-1$	$-m^2$	$im\sqrt{1-m^2}$	$6im\sqrt{1-m^2} - (2m^2 - 1)$
4	dn	m^2-1	$2-m^2$	-1	$\sqrt{1-m^2}$	$6\sqrt{1-m^2} - (2-m^2)$
5	sc	1	$2-m^2$	$1-m^2$	$\sqrt{1-m^2}$	$6\sqrt{1-m^2} - (2-m^2)$
6	sd	1	$2m^2-1$	$-m^2(1-m^2)$	$im\sqrt{1-m^2}$	$6im\sqrt{1-m^2} - (2m^2 - 1)$
7	ns + cs	$\frac{1}{4}$	$\frac{1}{2}(1-2m^2)$	$\frac{1}{4}$	$\frac{1}{4}$	$1 + m^2$
8	sn + i cn	$\frac{m^2}{4}$	$\frac{1}{2}(m^2-2)$	$\frac{m^2}{4}$	$\frac{m^2}{4}$	$1 + m^2$
9	cn/(1 + sn)	$\frac{1-m^2}{4}$	$\frac{1}{2}(1+m^2)$	$\frac{1-m^2}{4}$	$\frac{1-m^2}{4}$	$1 - 2m^2$
10	$m$sn + i dn	$\frac{1}{4}$	$\frac{1}{2}(1-2m^2)$	$\frac{1}{4}$	$\frac{1}{4}$	$1 + m^2$

This is an open access article under the CC BY-SA license.

Table 2. *Amplitudes of the ten oblique families from (12), with principal square roots; in every case* $U = c + g_1 F + f_1/F$, $\xi = x + \ell y - ct$, *and the last column gives the range of* m *on which the solution is real (under (H2)).*

Case	$F(\xi)$	g_1	f_1	real for
1	sn	$\tilde{c}\sqrt{2m^2/D}$	$\tilde{c}\sqrt{2/D}$	$0 < m < 1$
2	cd	$\tilde{c}\sqrt{2m^2/D}$	$\tilde{c}\sqrt{2/D}$	$0 < m < 1$
3	cn	$\tilde{c}\sqrt{-2m^2/D}$	$\tilde{c}\sqrt{2(1-m^2)/D}$	complex
4	dn	$\tilde{c}\sqrt{-2/D}$	$-\tilde{c}\sqrt{2(m^2-1)/D}$	$m^* < m < 1$
5	sc	$\tilde{c}\sqrt{2(1-m^2)/D}$	$\tilde{c}\sqrt{2/D}$	$0 < m < m^*$
6	sd	$\tilde{c}\sqrt{-2m^2(1-m^2)/D}$	$\tilde{c}\sqrt{2/D}$	complex
7	ns + cs	$\tilde{c}/\sqrt{2(1+m^2)}$	$\tilde{c}/\sqrt{2(1+m^2)}$	$0 < m < 1$
8	sn + i cn	$m\tilde{c}/\sqrt{2(1+m^2)}$	$m\tilde{c}/\sqrt{2(1+m^2)}$	complex (F complex)
9	cn/(1 + sn)	$\tilde{c}\sqrt{\dfrac{1-m^2}{2(1-2m^2)}}$	$\tilde{c}\sqrt{\dfrac{1-m^2}{2(1-2m^2)}}$	$0 < m < 1/\sqrt{2}$
10	$m$sn + i dn	$\tilde{c}/\sqrt{2(1+m^2)}$	$\tilde{c}/\sqrt{2(1+m^2)}$	complex (F complex)

We now give the complete closed form $U_i(\xi)$ and $U_i'(\xi)$ for all ten families explicitly, obtained from U_i, U_i' of Almasroub and Al-Naas Al-Wahishi (2026, Section 5) by the single replacement $c \mapsto \tilde{c}$ in g_1, f_1 (never in $g_0 = c$ itself), and with the sign of f_1 fixed by the product rule (12). In every case $U_i' = (g_1 - f_1/F^2)F'$.

Case 1 (real). $D = m^2 + 6m + 1$, $F = \mathrm{sn}$:

$$U_1 = c + \tilde{c}\sqrt{\frac{2}{D}}(m\,\mathrm{sn} + \mathrm{sn}^{-1}), \qquad U_1' = \tilde{c}\sqrt{\frac{2}{D}}\left(m - \frac{1}{\mathrm{sn}^2}\right)\mathrm{cn}\,\mathrm{dn}. \tag{16}$$

Case 2 (real). Same D, g_1, f_1 as Case 1, $F = \mathrm{cd}$:

$$U_2 = c + \tilde{c}\sqrt{\frac{2}{D}}(m\,\mathrm{cd} + \mathrm{dc}), \qquad U_2' = \tilde{c}\sqrt{\frac{2}{D}}(m - \mathrm{dc}^2)\left(-(1-m^2)\frac{\mathrm{sn}}{\mathrm{dn}^2}\right). \tag{17}$$

Case 3 (complex). $D = 6im\sqrt{1-m^2} - (2m^2 - 1)$, $F = \mathrm{cn}$:

$$U_3 = c + \tilde{c}\sqrt{\frac{-2m^2}{D}}\,\mathrm{cn} + \tilde{c}\sqrt{\frac{2(1-m^2)}{D}}\,\mathrm{cn}^{-1}, \qquad U_3' = \left(g_1 - \frac{f_1}{\mathrm{cn}^2}\right)(-\mathrm{sn}\,\mathrm{dn}). \tag{18}$$

Case 4 (complex for $0 < m < m^*$; real for $m^* < m < 1$). $D = 6\sqrt{1-m^2} - (2 - m^2)$, $F = \mathrm{dn}$:

$$U_4 = c + \tilde{c}\sqrt{\frac{-2}{D}}\,\mathrm{dn} - \tilde{c}\sqrt{\frac{2(m^2-1)}{D}}\,\mathrm{dn}^{-1}, \qquad U_4' = \left(g_1 - \frac{f_1}{\mathrm{dn}^2}\right)(-m^2\,\mathrm{sn}\,\mathrm{cn}). \tag{19}$$

This is an open access article under the CC BY-SA license.

The minus sign in f_1 holds on the whole range $0 < m < 1$, $m \neq m^*$. On the real branch $m^* < m < 1$ ($D < 0$) it coincides with the sign $\varepsilon = \operatorname{sign}(D) = -1$ of (Almasroub & Al-Naas Al-Wahishi, 2026); on the complex branch $0 < m < m^*$ ($D > 0$) both principal roots are imaginary, and the product rule again requires the minus sign, whereas $\varepsilon = \operatorname{sign}(D) = +1$ would reverse the sign of $g_1 f_1$ (Remark 3) and leave a residual of order 10^{-1} in (5). The real branch is the family checked in detail in Check 2 of Section 5.

Case 5 (real for $0 < m < m^*$). Same D as Case 4, $F = \mathrm{sc}$:

$$U_5 = c + \tilde{c}\sqrt{\frac{2(1-m^2)}{D}}\,\mathrm{sc} + \tilde{c}\sqrt{\frac{2}{D}}\,\mathrm{cs}, \qquad U_5{}' = \left(g_1 - \frac{f_1}{\mathrm{sc}^2}\right)\mathrm{dc}\,\mathrm{nc}. \tag{20}$$

Case 6 (complex). Same D as Case 3, $F = \mathrm{sd}$:

$$U_6 = c + \tilde{c}\sqrt{\frac{-2m^2(1-m^2)}{D}}\,\mathrm{sd} + \tilde{c}\sqrt{\frac{2}{D}}\,\mathrm{ds}, \qquad U_6{}' = \left(g_1 - \frac{f_1}{\mathrm{sd}^2}\right)\mathrm{cd}\,\mathrm{nd}. \tag{21}$$

Case 7 (real). $D = 1 + m^2$, $g_1 = f_1 = \tilde{c}/\sqrt{2(1+m^2)}$, $F = \mathrm{ns} + \mathrm{cs}$ (equivalently, via Table 2 of (Almasroub & Al-Naas Al-Wahishi, 2026), $F = \mathrm{sn}/(1 + \mathrm{cn})$, used in Figure 4); since $F' = -\mathrm{ds} \cdot F$:

$$U_7 = c + \frac{\tilde{c}}{\sqrt{2(1+m^2)}}\left(F + \frac{1}{F}\right), \qquad U_7{}' = \frac{\tilde{c}}{\sqrt{2(1+m^2)}}\left(1 - \frac{1}{F^2}\right)(-\mathrm{ds} \cdot F). \tag{22}$$

Case 8 (complex; F itself complex). $D = 1 + m^2$, $g_1 = f_1 = m\tilde{c}/\sqrt{2(1+m^2)}$, $F = \mathrm{sn} + i\,\mathrm{cn}$; since $F' = -i\,\mathrm{dn} \cdot F$:

$$U_8 = c + \frac{m\tilde{c}}{\sqrt{2(1+m^2)}}\left(F + \frac{1}{F}\right), \qquad U_8{}' = \frac{m\tilde{c}}{\sqrt{2(1+m^2)}}\left(1 - \frac{1}{F^2}\right)(-i\,\mathrm{dn} \cdot F). \tag{23}$$

Case 9 (real for $0 < m < 1/\sqrt{2}$). $D = 1 - 2m^2$, $F = \mathrm{cn}/(1 + \mathrm{sn})$, and

$$g_1 = f_1 = \tilde{c}\sqrt{\frac{1-m^2}{2(1-2m^2)}} \qquad \text{(the denominator } 1 - 2m^2 \text{ is not squared)}, \tag{24}$$

$$U_9 = c + g_1\left(F + \frac{1}{F}\right), \qquad U_9{}' = g_1\left(1 - \frac{1}{F^2}\right)\left(-\frac{\mathrm{dn}}{1+\mathrm{sn}}\right). \tag{25}$$

Case 10 (complex; F itself complex). $D = 1 + m^2$, $g_1 = f_1 = \tilde{c}/\sqrt{2(1+m^2)}$, $F = m\,\mathrm{sn} + i\,\mathrm{dn}$:

$$U_{10} = c + \frac{\tilde{c}}{\sqrt{2(1+m^2)}}\left(F + \frac{1}{F}\right), \qquad U_{10}{}' = \frac{\tilde{c}}{\sqrt{2(1+m^2)}}\left(1 - \frac{1}{F^2}\right) m\,\mathrm{cn}(\mathrm{dn} - i\,m\,\mathrm{sn}). \tag{26}$$

In every case $V_i(\xi) = c\,U_i(\xi) - \frac{1}{2}U_i^2(\xi) - b\,U_i{}'(\xi) + C_1$ (the original C_1, not $C_1{}'$), and the domain excludes the zeros of $F(\xi)$ together with any point where $F(\xi)$ itself is undefined (e.g. $\mathrm{sn} = 0$ for Case 7's $F = \mathrm{ns} + \mathrm{cs}$, or $\mathrm{sn} = -1$ for Case 9's $F = \mathrm{cn}/(1 + \mathrm{sn})$), exactly as in Almasroub and Al-Naas Al-Wahishi (2026, Remark 6). Setting $\ell = 0$ in every formula above gives $\tilde{c} \to \sqrt{c^2 + 2C_1}$, recovering every $U_i, U_i{}'$ of Almasroub and Al-Naas Al-Wahishi (2026,

This is an open access article under the CC BY-SA license.

Section 5) (with the Case-4 sign as in (19)); setting further $C_1 = 0$ recovers the base families of Almasroub and Al-Naas Al-Wahishi (2026, Table 1).

5 Verification Against the Original PDE System

We verify Theorem 1 at the level of the original, unintegrated system – treating x, y, t as independent variables and differentiating the fields $u(x, y, t) = U(x + \ell y - ct)$ and v from (8) directly, rather than checking only the reduced ODE (10). All computations use 50-significant-digit precision (mpmath, Python; derivatives via mpmath.diff's internal high-order extrapolation). We denote by R_1 the left-hand side of (3) and by R_2 that of (4), or of its local form (5) where stated; the latter avoids the nonlocal operator altogether and is therefore an independent check of Lemma 1.

5.1 Two detailed checks

Check 1: Case 1 ($D > 0$), genuine transverse dependence. Take Case 1 ($F = \mathrm{sn}$, $l_0 = 1$, $l_1 = -(1 + m^2)$, $l_2 = m^2$, $D = m^2 + 6m + 1$) with $m = 0.5$, $c = 1.5$, $b = 0.6$, $C_1 = 0.3$, $\sigma = +1$, $\ell = 0.4$. Then $D = 4.25$, $C_1' = C_1 + \sigma\ell^2 = 0.46$, $\tilde{c} = \sqrt{c^2 + 2C_1'} \approx 1.78045$, $a + b^2 \approx 0.37294$ so $a \approx 0.01294$, $g_1 \approx 0.61069$, $f_1 \approx 1.22138$, $C_2 = -cC_1' = -0.69$. At $(x, y, t) = (0.9, 0.5, 0.2)$, with $U = c + g_1 \mathrm{sn}(\xi, m) + f_1/\mathrm{sn}(\xi, m)$ and V from (8) (using $C_1 = 0.3$, not C_1'),

$$R_1 \approx 5.35 \times 10^{-51}, \qquad R_2 \approx 4.01 \times 10^{-51}, \tag{27}$$

i.e. both original PDEs (3)–(4) are satisfied to full working precision. As an independent consistency check on the realization (7) itself, direct numerical differentiation gives $u_{yy}(x, y, t) - \ell^2 U''(\xi) \approx 1.34 \times 10^{-51}$ at the same point, and the local form (5) gives $|R_2| \approx 1.2 \times 10^{-49}$.

Check 2: Case 4 ($D < 0$, real branch), opposite sign $\sigma = -1$. Take Case 4 ($F = \mathrm{dn}$, $l_0 = m^2 - 1$, $l_1 = 2 - m^2$, $l_2 = -1$, $D = 6\sqrt{1 - m^2} - (2 - m^2)$) with $m = 0.99 > m^*$ (so $D < 0$), $c = 1$, $b = 0.6$, $C_1 = 0.2$, $\sigma = -1$, $\ell = 0.3$. Then $D \approx -0.17350$, $C_1' = C_1 + \sigma\ell^2 = 0.11$, $\tilde{c}^2 = c^2 + 2C_1' = 1.22$, $a + b^2 \approx -3.51593$ so $a \approx -3.87593$, $g_1 \approx 3.75017$, $f_1 = -\tilde{c}\sqrt{2l_0/D} \approx -0.52903$ (the minus sign of (19)), $C_2 = -cC_1' = -0.11$. At $(x, y, t) = (0.7, 0.4, 0.1)$, with $U = c + g_1 \mathrm{dn}(\xi, m) + f_1/\mathrm{dn}(\xi, m)$,

$$R_1 \approx 1.34 \times 10^{-50}, \qquad R_2 \approx -7.12 \times 10^{-50}, \tag{28}$$

again satisfied to full working precision. This confirms that Theorem 1 correctly inherits the sign structure required on the real branch of Case 4 under genuine, non-zero transverse dependence ($\ell \neq 0$) and with the opposite KP sign from Check 1.

5.2 Systematic multi-period grid scan

Two isolated points cannot exclude a defect located elsewhere on the solution, nor one affecting only some families. We therefore scanned all ten families (Case 4 on both branches, $m = 0.5 <$

This is an open access article under the CC BY-SA license.

m^* and $m = 0.99 > m^*$), for *both* signs $\sigma = \pm 1$, with $c = 1.5$, $b = 0.6$, $C_1 = 0.3$, $\ell = 0.4$, $m = 0.5$ unless stated, and a fixed by (H3). For each configuration, 24 points (x, y, t) were drawn with $\xi = x + \ell y - ct$ uniformly distributed over three full periods, $\xi \in [-6K(m), 6K(m)]$, $y \in [-2,2]$, $t \in [0,1]$; points within 10^{-2} of a zero or pole of F (or of $\mathrm{sn} = 0$, $\mathrm{sn} = -1$ for Cases 7 and 9) were rejected. At each point we evaluated R_1, the residual R_2 of the local form (5), and the error of the printed derivative formula U_i' against numerical differentiation. The maxima over each scan are reported in Table 3.

Table 3. *Multi-period grid scan (24 points over three periods per row, 50-digit arithmetic): maximum absolute residuals of (3) and of the local form (5), maximum error of the printed derivative U_i', and maximum $|U|$ on the sample.*

Case	m	σ	$\max\|R_1\|$	$\max\|R_2\|$	$\max\|U_i' - U'_{\mathrm{num}}\|$	$\max\|U\|$
1	0.5	+1	5.3×10^{-45}	4.9×10^{-43}	8.2×10^{-48}	37.5
1	0.5	−1	3.4×10^{-48}	1.6×10^{-46}	2.1×10^{-50}	4.6
2	0.5	+1	1.0×10^{-48}	1.1×10^{-46}	4.3×10^{-50}	5.5
2	0.5	−1	4.9×10^{-44}	8.6×10^{-42}	5.5×10^{-48}	49.7
3	0.5	+1	8.7×10^{-48}	1.7×10^{-45}	1.9×10^{-49}	14.9
3	0.5	−1	2.3×10^{-47}	2.7×10^{-45}	2.4×10^{-49}	11.1
4	0.5	+1	1.5×10^{-51}	3.7×10^{-51}	6.7×10^{-52}	1.5
4	0.5	−1	1.0×10^{-51}	3.8×10^{-51}	6.7×10^{-52}	1.5
4	0.99	+1	1.4×10^{-48}	9.9×10^{-48}	4.9×10^{-49}	6.7
4	0.99	−1	1.0×10^{-48}	5.7×10^{-48}	2.2×10^{-49}	6.1
5	0.5	+1	6.3×10^{-46}	1.3×10^{-43}	1.4×10^{-48}	27.4
5	0.5	−1	4.8×10^{-44}	5.6×10^{-41}	1.4×10^{-48}	78.5
6	0.5	+1	4.2×10^{-46}	1.2×10^{-43}	6.8×10^{-49}	24.6
6	0.5	−1	6.2×10^{-46}	8.0×10^{-43}	2.7×10^{-48}	42.8
7	0.5	+1	4.4×10^{-44}	1.0×10^{-42}	7.3×10^{-46}	60.7
7	0.5	−1	2.2×10^{-46}	1.5×10^{-44}	1.3×10^{-47}	22.3
8	0.5	+1	8.8×10^{-51}	5.5×10^{-51}	2.7×10^{-51}	2.6
8	0.5	−1	8.7×10^{-51}	3.5×10^{-51}	2.7×10^{-51}	2.5
9	0.5	+1	3.8×10^{-47}	2.7×10^{-45}	5.1×10^{-49}	21.6
9	0.5	−1	1.6×10^{-45}	3.0×10^{-43}	1.4×10^{-48}	42.8
10	0.5	+1	6.4×10^{-51}	4.8×10^{-51}	2.7×10^{-51}	2.6
10	0.5	−1	8.9×10^{-51}	6.0×10^{-51}	2.7×10^{-51}	2.5

All 22 scans (528 points) satisfy the full PDE system to within 6×10^{-41}, and all printed derivatives U_i' (after the corrections in (22), (23)) agree with numerical differentiation to within 10^{-45}. The spread of the residuals over ten orders of magnitude is not a property of the solutions but of the numerical differentiation: the largest residuals occur in the rows with the largest $|U|$, i.e. at sample points close to a pole of F or $1/F$, where the fourth-order mixed derivatives in (5) are large and the extrapolation error grows accordingly; the pole-free complex families (Cases 4 at $m = 0.5, 8, 10$) stay at the 10^{-51} level throughout. The same scan was also used as a negative control: replacing the product rule by $\varepsilon = \mathrm{sign}(D)$ on the complex branch of Case 4 ($m = 0.5$)

This is an open access article under the CC BY-SA license.

gives $|R_2| \approx 0.2$; using a squared denominator $(1-2m^2)^2$ in (24) gives $|R_2| \approx 5\times 10^2$; and omitting the factor F in ${U_7}'$, ${U_8}'$ gives derivative errors of 2.3 and 0.67, respectively. These controls show that the scan is sensitive to exactly the kinds of error that it rules out.

6 Physical Reading and Representative Profiles

The oblique variable $\xi = x + \ell y - ct$ describes a plane wavefront propagating in the x-direction at speed c, whose crests are the lines $x + \ell y =$ const, of slope $-1/\ell$ in the (x, y)-plane – equivalently, the wave normal $(1, \ell)$ makes the angle $\arctan\ell$ with the x-axis and the crest lines make the same angle with the y-axis, exactly as for oblique solutions of the KP equation itself. Figure 1 shows this directly for Case 1 at $m = 0.5$, $c = 1.5$, $\ell = 0.45$, $\sigma = +1$, $C_1 = 0$ (so ${C_1}' = \sigma\ell^2 = 0.2025$): the left panel is the profile $U(\xi)$; the right panel is the field $u(x, y, 0)$ over the (x, y)-plane, showing the pole lattice of Case 1 as a family of parallel oblique wavefronts – the genuinely two-dimensional content of Theorem 1 that has no counterpart in (Almasroub & Al-Naas Al-Wahishi, 2026).

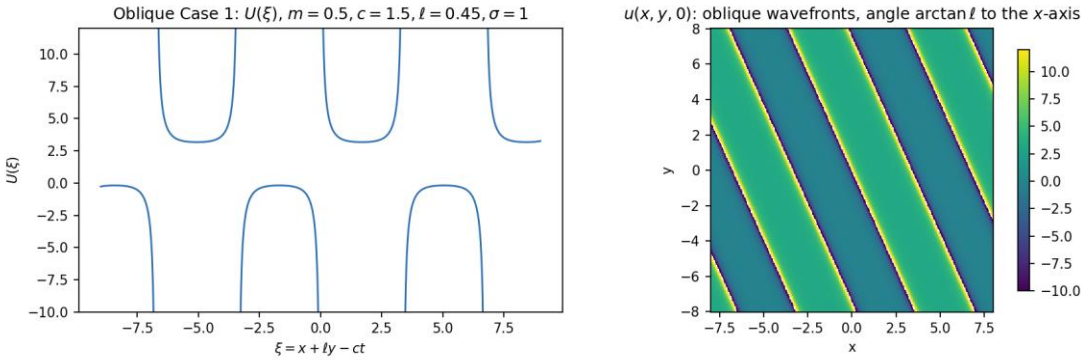

Figure 1. *Oblique extension of Case 1 ($m = 0.5$, $c = 1.5$, $\ell = 0.45$, $\sigma = +1$, $C_1 = 0$). Left: the profile $U(\xi)$ against $\xi = x + \ell y - ct$. Right: the field $u(x, y, 0)$ over the (x, y)-plane, showing the pole lattice of Case 1 as parallel oblique wavefronts whose normal makes the angle $\arctan\ell = \arctan 0.45 \approx 24.2°$ with the x-axis.*

To parallel Section 7 of (Almasroub & Al-Naas Al-Wahishi, 2026) directly, we display the oblique extension of the same four representative cases used there, all with $\ell = 0.4$, $\sigma = +1$, $C_1 = 0$ (so ${C_1}' = \sigma\ell^2 = 0.16$, $\tilde{c} = \sqrt{c^2 + 0.32}$), each shown as a profile $U(\xi)$ next to the corresponding (x, y)-plane field at $t = 0$.

Figure 2 (near-trigonometric branch, oblique Case 1, $m = 0.05$). As $m \to 0$ the family approaches the singular periodic train $U_1 \to c + \sqrt{2}\,\tilde{c}\csc\xi$, now propagating obliquely.

Figure 3 (solitary limit, oblique Case 1, $m \to 1$). Exactly as in Almasroub and Al-Naas Al-Wahishi (2026, Section 7), the family itself remains singular as $m \to 1$: since $\mathrm{sn}(\xi, m) \to \tanh\xi$ but $\mathrm{sn}^{-1}(\xi, m) \to \coth\xi$ diverges at $\xi = 0$, only the degenerate branch $f_1 = 0$ is smooth. For $F = \tanh\xi$ ($l_0 = 1$, $l_1 = -2$, $l_2 = 1$) the conditions in the proof of Theorem 1 with $f_1 = 0$ give $g_1 = \tilde{c}$ and $a + b^2 = \tilde{c}^{\,2}/4$, so that this degenerate branch is the smooth oblique kink $U = c +$

This is an open access article under the CC BY-SA license.

$\tilde{c}\tanh\xi$, connecting $c-\tilde{c}$ to $c+\tilde{c}$; it is plotted (dashed) for comparison in the left panel, and visibly coincides with the outer parts of the singular family at $m=0.999$, the two differing only in a neighbourhood of the pole. The right panel shows the singular family's single oblique wavefront (pole line) in the (x,y)-plane.

Figure 4 (composite rational train, oblique Case 7). Case 7 shown via its equivalent form $F=\mathrm{sn}/(1+\mathrm{cn})$ (Table 2 of (Almasroub & Al-Naas Al-Wahishi, 2026)), $m=0.5$: the half-argument, multi-crest structure of Almasroub and Al-Naas Al-Wahishi (2026, Remark 8) now propagates obliquely as a family of parallel multi-crest wavefronts.

Figure 5 (localized trough packet, oblique Case 2). Case 2 with $F=\mathrm{cd}$, $m=0.85$, $c=1.4$.

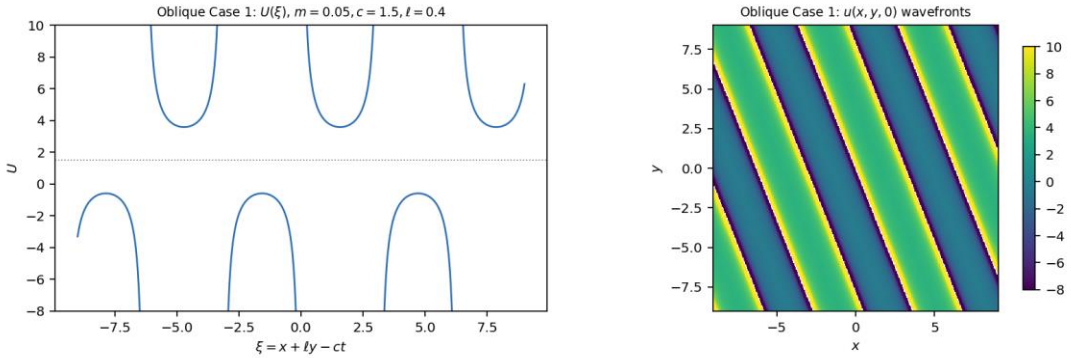

Figure 2. *Oblique Case 1, near-trigonometric branch, $m=0.05$, $c=1.5$, $\ell=0.4$. Left: profile $U(\xi)$. Right: $u(x,y,0)$ wavefronts.*

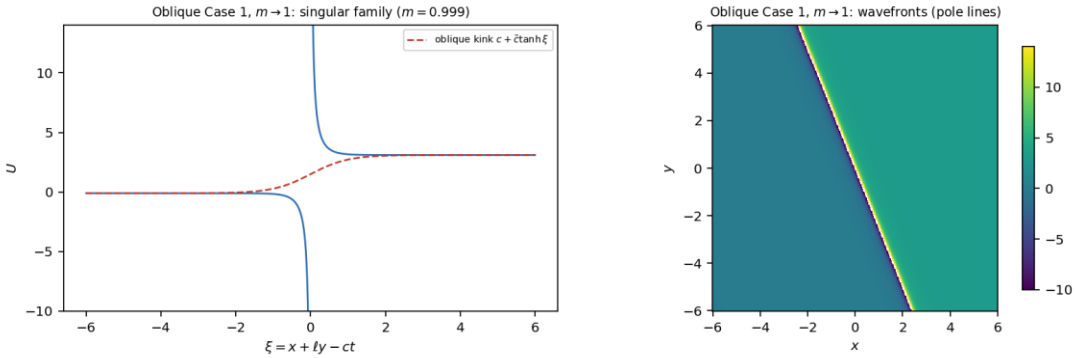

Figure 3. *Oblique Case 1 as $m\to 1$ ($m=0.999$, $c=1.5$, $\ell=0.4$). Left: the singular family (solid) versus the distinct smooth oblique kink $U=c+\tilde{c}\tanh\xi$ (dashed; the $f_1=0$ degenerate branch, with its own $a+b^2=\tilde{c}^{\,2}/4$). Right: the singular family's wavefront (pole line) in the (x,y)-plane.*

This is an open access article under the CC BY-SA license.

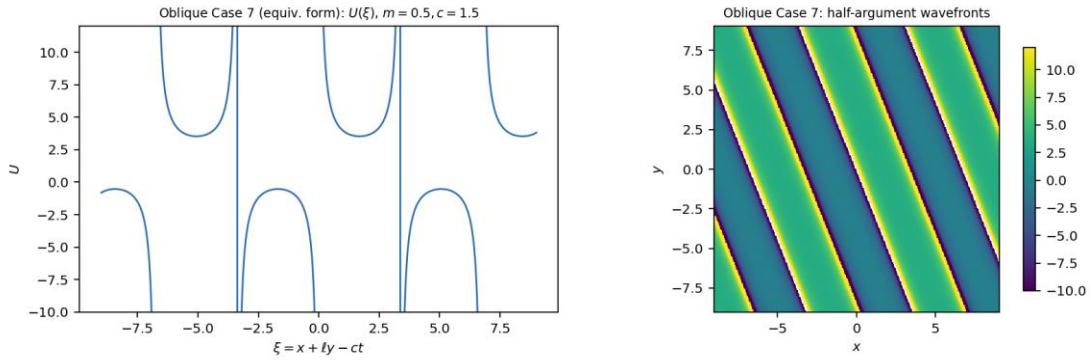

Figure 4. *Oblique Case 7 (equivalent form* $F = \mathrm{sn}/(1 + \mathrm{cn})$*), composite rational periodic train,* $m = 0.5$*,* $c = 1.5$*,* $\ell = 0.4$*. Left: profile* $U(\xi)$*. Right: half-argument multi-crest wavefronts.*

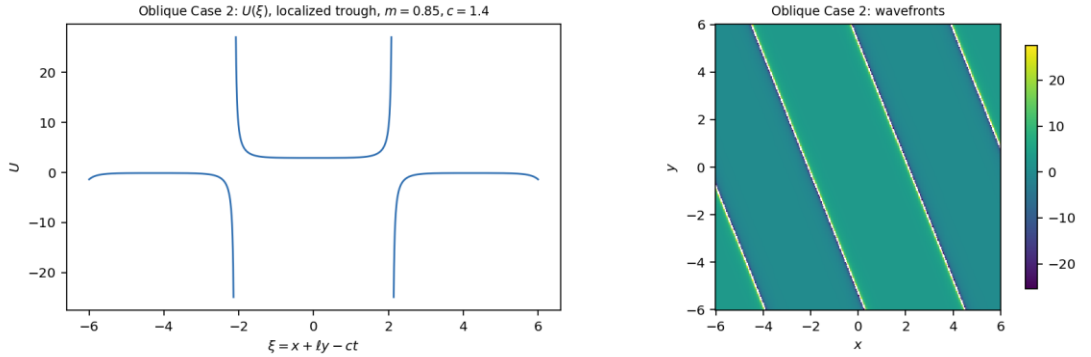

Figure 5. *Oblique Case 2, localized trough packet,* $m = 0.85$*,* $c = 1.4$*,* $\ell = 0.4$*. Left: profile* $U(\xi)$*. Right:* $u(x, y, 0)$ *wavefronts.*

Remark 6 (Scope). As in (Almasroub & Al-Naas Al-Wahishi, 2026), no claim of dynamical or spectral stability is made for these profiles, and none is implied by the high-precision verification of Section 5, which establishes that the stated closed forms satisfy the stated PDE system at all sampled points of the multi-period scan (together with the exact symbolic reduction of Theorem 1). We also do not claim that the system (3)–(4) is integrable, nor that it coincides with any of the specific $(2 + 1)$-dimensional WBK systems of Zheng et al. (2005), Ali and Younas (2025), or Pashaev and Rogers (2025); it is offered as an explicit, self-consistent, and now fully solved extension, in the same spirit that the KP equation extends KdV.

7 Conclusion

We defined a specific, self-contained, anisotropic $(2 + 1)$-dimensional Kadomtsev–Petviashvili-type extension of the Whitham–Broer–Kaup system studied in (Almasroub & Al-Naas Al-Wahishi, 2026), with a precise functional definition of its nonlocal term and a weakly-transverse motivation for placing that term in the mass balance, and showed (Theorem 1) that its oblique traveling-wave reduction is governed by exactly the same second-order ODE already

This is an open access article under the CC BY-SA license.

solved there, under the substitution $C_1 \mapsto C_1' = C_1 + \sigma\ell^2$. This is not an analogy: the reduced ODE is identical term for term, so every one of the ten independent Jacobi-elliptic families of (Almasroub & Al-Naas Al-Wahishi, 2026) extends immediately, without new algebra, to an exact $(2+1)$-dimensional oblique solution, under the explicit admissibility conditions (H1)–(H3) – in particular $\ell^2 < (c^2 + 2C_1)/2$ when $\sigma = -1$. Writing the amplitude condition in the branch-independent product form $g_1 f_1 = 2\tilde{c}^{\,2}\sqrt{l_0 l_2}/D$ fixes the sign of the complex branch of Case 4. All ten families were verified to 50-digit precision directly against the original, unintegrated PDE system by a multi-period grid scan for both KP signs. Setting the transverse wavenumber $\ell = 0$ recovers every result of (Almasroub & Al-Naas Al-Wahishi, 2026) exactly. Directions left for future work include the analogous extension of the universal Weierstrass representation and of the general-C_1 theorem's degenerate branches to this $(2+1)$-dimensional setting; the regime $\tilde{c}^{\,2} < 0$ (Remark 5); the kink-type solutions of the alternative placement (Appendix A); genuinely non-planar (non-oblique) solutions of (3)–(4), such as interacting oblique waves; a comparison, at the level of exact solutions, with the specific constructions of Zheng et al. (2005), Ali and Younas (2025) and Pashaev and Rogers (2025); and – to strengthen the physical relevance of the classification – a linear and transverse stability analysis of the real families, for which the explicit closed forms obtained here provide exact base states and benchmark solutions for numerical solvers.

Appendix A. The alternative placement of the transverse term

For completeness we record what happens if the nonlocal term is placed in the momentum equation instead, i.e. for the system

$$u_t + u\,u_x + v_x + b\,u_{xx} + \sigma\,\partial_x^{-1}u_{yy} = 0, \qquad v_t + (uv)_x + a\,u_{xxx} - b\,v_{xx} = 0, \quad (29)$$

with ∂_x^{-1} as in Proposition 1. Under (6) and Lemma 1, the first equation integrates to

$$V = K\,U - \tfrac{1}{2}U^2 - b\,U' + C_1, \qquad K := c - \sigma\ell^2, \quad (30)$$

and substituting into the second equation and integrating once gives (symbolically verified)

$$(a+b^2)\,U'' + b\sigma\ell^2\,U' - \tfrac{1}{2}U^3 + \left(\tfrac{3}{2}c - \sigma\ell^2\right)U^2 + (C_1 - c^2 + c\sigma\ell^2)U + C_2 = 0, \quad (31)$$

the constant $-cC_1$ having been absorbed into C_2. Since $c - K = \sigma\ell^2$, the new first-derivative term is $b(c-K)U' = b\sigma\ell^2 U'$; but, unlike in Theorem 1, the coefficients of U^2 and U are modified as well, and K depends on c, σ and ℓ together.

Proposition 2 (Parity obstruction). If $b\sigma\ell^2 \neq 0$, equation (31) has no non-constant solution of the form $U = c_0 + g_1 F + f_1/F$ in which F is a non-constant elliptic function satisfying $F'^2 = l_0 + l_1 F^2 + l_2 F^4$.

Proof. Using $F'' = l_1 F + 2l_2 F^3$ and $F'^2 = P(F) := l_0 + l_1 F^2 + l_2 F^4$, the terms U'', U^3, U^2, U and C_2 of (31) are rational functions $R(F)$ of F alone (they contain only even powers of F'), whereas $U' = G(F)\,F'$ with $G(F) = g_1 - f_1/F^2$ is linear in F'. Thus (31) reads $R(F) +$

This is an open access article under the CC BY-SA license.

$b\sigma\ell^2\, G(F)\, F' = 0$. Since F' is a non-constant elliptic function it has a zero ξ_0, and because the equation $F'' = \frac{1}{2}P'(F)$ is autonomous and reversible, uniqueness of its initial-value problem gives $F(\xi_0 + s) = F(\xi_0 - s)$; hence F is even and F' odd about ξ_0. Then $R(F)$ is even and $G(F)F'$ odd about ξ_0, so both must vanish identically; as $F' \not\equiv 0$, $G(F) \equiv 0$, i.e. $g_1 = f_1 = 0$ and $U \equiv c_0$. ▫

The obstruction disappears in the degenerate (hyperbolic) limits, where F' has no zero. Indeed, a direct substitution shows that (31) admits the Huxley-type front

$$U = \alpha + \beta\tanh(\kappa\xi), \qquad \beta = 2\kappa\sqrt{a+b^2}, \qquad \alpha = c - \frac{2}{3}\sigma\ell^2 - \frac{b\sigma\ell^2}{3\sqrt{a+b^2}}, \tag{32}$$

for any $\kappa > 0$ and $a + b^2 > 0$, provided C_1 and C_2 take the values fixed by the remaining two coefficient conditions, namely $C_1 - c^2 + c\sigma\ell^2 = \frac{1}{2}\left[4(a+b^2)\kappa^2 + 3\alpha^2 - 4\alpha\left(\frac{3}{2}c - \sigma\ell^2\right)\right]$ and $C_2 = \frac{1}{2}\left[\alpha^3 - 2\alpha^2\left(\frac{3}{2}c - \sigma\ell^2\right) - 2\alpha(C_1 - c^2 + c\sigma\ell^2) - 2b\sigma\ell^2\beta\kappa\right]$ (verified symbolically, e.g. for $c = \frac{3}{2}$, $b = \frac{3}{5}$, $\sigma = 1$, $\ell = \frac{2}{5}$, $a + b^2 = \frac{1}{2}$, $\kappa = \frac{1}{2}$). Equation (31) is thus amenable to tanh/Riccati-type, first-integral or Painlevé-type approaches, whose auxiliary functions are not restricted by the parity argument above; a systematic treatment of (29) along these lines is left for future work.

References

Abdoon, M. A. (2015). First integral method: A general formula for nonlinear fractional Klein–Gordon equation using advanced computing language. *Computational Methods*, 127–134.

Ablowitz, M. J., & Segur, H. (1979). On the evolution of packets of water waves. *Journal of Fluid Mechanics, 92*(4), 691–715.

Ali, A., & Younas, U. (2025). Multi-soliton interactions and periodic wave patterns for the (2+1)-dimensional coupled Whitham–Broer–Kaup system. *Physica Scripta, 100*(3), Article 035211.

Almasroub, R. M. A., & Al-Naas Al-Wahishi, R. M. (2026). Construction and classification of exact Jacobi elliptic traveling-wave solutions for the coupled Whitham–Broer–Kaup system via the generalized F-expansion method. *Rawafed Almarefa Journal, 7*(13), 50–75.

Almasroub, R. M. A., Khalaf, L. A., & Al-Tawil, A. A. A. (2020). Constructing exact solutions of the Burgers–Huxley equation via (G'/G)-expansion method. *Rawafed Almarefa Journal, 6*(12), 33–53.

Al-shawba, A. A., Abdullah, F. A., Gepreel, K. A., & Azmi, A. (2018). Solitary and periodic wave solutions of higher-dimensional conformable time-fractional differential equations using the $(G'/G, 1/G)$-expansion method. *Advances in Difference Equations, 2018*(1), Article 149.

Chen, Y., Wang, Q., & Li, B. (2005). Elliptic equation rational expansion method and new exact travelling solutions for Whitham–Broer–Kaup equations. *Chaos, Solitons & Fractals, 26*(1), 231–246.

This is an open access article under the CC BY-SA license.

Davey, A., & Stewartson, K. (1974). On three-dimensional packets of surface waves. *Proceedings of the Royal Society of London. Series A, 338*, 101–110.

El-Borai, M. M., & Al-Masroub, R. M. (2015). Exact solutions for some nonlinear parabolic equations. *International Journal of Mathematics and Computer Applications Research, 10*, 106–122.

El-Borai, M. M., El-Sayed, W. G., & Al-Masroub, R. M. (2015). Exact solutions for time fractional coupled Whitham–Broer–Kaup equations via Exp-function method. *International Research Journal of Engineering and Technology, 2*(6), 307–315.

El-Borai, M. M., El-Sayed, W. G., & Al-Masroub, R. M. (2016). Exact solutions of some nonlinear partial differential equations via extended method. *Journal of Advances in Mathematics, 36*(1), 60–71.

El-Sabbagh, M. F., & El-Ganaini, S. I. A. (2012). New exact solutions of Broer–Kaup (BK) and Whitham–Broer–Kaup (WBK) systems via the first integral method. *International Journal of Mathematical Analysis, 6*(46), 2287–2298.

Freeman, N. C., & Nimmo, J. J. C. (1983). Soliton solutions of the Korteweg–de Vries and Kadomtsev–Petviashvili equations: the Wronskian technique. *Physics Letters A, 95*(1), 1–3.

Gepreel, K. A. (2014). Explicit Jacobi elliptic exact solutions for nonlinear partial fractional differential equations. *Applied Mathematical Modelling, 38*(1), 1–14.

He, J. (2013). Exp-function method for fractional differential equations. *International Journal of Nonlinear Sciences and Numerical Simulation, 14*(6), 363–366.

Hirota, R. (2004). *The direct method in soliton theory*. Cambridge University Press.

Kadomtsev, B. B., & Petviashvili, V. I. (1970). On the stability of solitary waves in weakly dispersive media. *Soviet Physics Doklady, 15*, 539–541.

Kaup, D. J. (1975). A higher-order water-wave equation and the method for solving it. *Progress of Theoretical Physics, 54*(2), 396–408.

Kodama, Y. (2010). KP solitons in shallow water. *Journal of Physics A: Mathematical and Theoretical, 43*(43), Article 434004.

Kumar, H., & Chand, F. (2014). Exact traveling wave solutions of some nonlinear evolution equations. *SpringerPlus, 3*(1), Article 456.

Li, W., Yang, H., & He, B. (2014). Exact solutions of fractional Burgers and Cahn–Hilliard equations using extended fractional Riccati expansion method. *Abstract and Applied Analysis, 2014*, Article 913840.

Maruno, K., Ankiewicz, A., & Akhmediev, N. (2003). Exact localized and periodic solutions of the discrete complex Ginzburg–Landau equation. *Optics Communications, 221*(1–3), 199–209.

Matveev, V. B., & Salle, M. A. (1991). *Darboux transformations and solitons*. Springer.

Parkes, E. J. (2010). Observations on the tanh–coth expansion method for finding solutions to nonlinear evolution equations. *Applied Mathematics and Computation, 217*(4), 1749–1754.

This is an open access article under the CC BY-SA license.

Pashaev, O. K., & Rogers, C. (2025). *Whitham–Broer–Kaup systems in multi-dimensions: Quantum and resonant NLS connections* [Preprint]. arXiv. https://arxiv.org/abs/2508.00660

Satsuma, J., & Ablowitz, M. J. (1979). Two-dimensional lumps in nonlinear dispersive systems. *Journal of Mathematical Physics, 20*(7), 1496–1503.

Seadawy, A. R., Cheemaa, N., & Albarakati, W. A. (2025). Dispersive optical solitary waves and closed-form solutions for the (2+1)-dimensional shallow water equations. *Results in Physics, 69*, Article 108112.

Wazwaz, A. M. (2007). The tanh–coth method for solitons and kink solutions for nonlinear parabolic equations. *Applied Mathematics and Computation, 188*(2), 1467–1475.

Whitham, G. B. (1974). *Linear and nonlinear waves*. Wiley.

Zayed, E. M. E., & Alurrfi, K. A. E. (2014). Solving two higher order nonlinear evolution equations. *Journal of Applied Mathematics, 2014*, Article 762149.

Zayed, E. M. E., & Alurrfi, K. A. E. (2015). The modified Kudryashov method for solving some seventh order nonlinear PDEs in mathematical physics. *Zeitschrift für Naturforschung A, 70*(4), 308–319.

Zerarka, A., Ouamane, S., & Attaf, A. (2010). On the functional variable method for finding exact solutions to a class of wave equations. *Applied Mathematics and Computation, 217*(2), 897–904.

Zerarka, A., Ouamane, S., & Attaf, A. (2016). Applications of the functional variable method for finding the exact solutions of nonlinear evolution equations in mathematical physics. *AIP Conference Proceedings, 1734*, Article 040001.

Zhang, Z., Yong, X., & Chen, Y. (2008). Symmetry analysis for Whitham–Broer–Kaup equations. *Journal of Nonlinear Mathematical Physics, 15*(4), 383–397.

Zheng, B. (2013). Exact solutions for some fractional partial differential equations by the (G'/G)-expansion method. *Mathematical Problems in Engineering, 2013*, Article 432757.

Zheng, C.-L., Zhu, H.-P., & Chen, L.-Q. (2005). Exact solution and semifolded structures of generalized Broer–Kaup system in (2+1)-dimensions. *Chaos, Solitons & Fractals, 26*(1), 187–194.

This is an open access article under the CC BY-SA license.